ORIGINAL RESEARCH PAPER

Development and analysis of a Bayesian water balance model for large lake systems

Joeseph. P. Smith[a] and Andrew. D. Gronewold[b,c]

[a]Cooperative Institute for Great Lakes Research (CIGLR), University of Michigan, Ann Arbor, Michigan USA, 48109; ORCID: 0000-0002-1896-1390 [b]Great Lakes Environmental Research Laboratory, National Oceanic and Atmospheric Administration, Ann Arbor, Michigan, USA, 48108; [c]Department of Civil and Environmental Engineering, University of Michigan, Ann Arbor, Michigan USA, 48109;

ABSTRACT

Water balance models (WBMs) are often employed to understand regional hydrologic cycles over various time scales. Most WBMs, however, are physically-based, and few employ state-of-the-art statistical methods to reconcile independent input measurement uncertainty and bias. Further, few WBMs exist for large lakes, and most large lake WBMs perform additive accounting, with minimal consideration towards input data uncertainty. Here, we introduce a framework for improving a previously developed large lake statistical water balance model (L2SWBM). Focusing on the water balances of Lakes Superior and Michigan-Huron, we demonstrate our new analytical framework, identifying L2SWBMs from 26 alternatives that adequately close the water balance of the lakes with satisfactory computation times compared with the prototype model. We expect our new framework will be used to develop water balance models for other lakes around the world.

1. Introduction

As global freshwater demand increases [51, 76], there is a growing need for a comprehensive understanding of changes and drivers of hydrologic cycles over a wide variety of hydrologic systems [9, 34, 42, 49, 75]. Water balance models (WBMs) are often
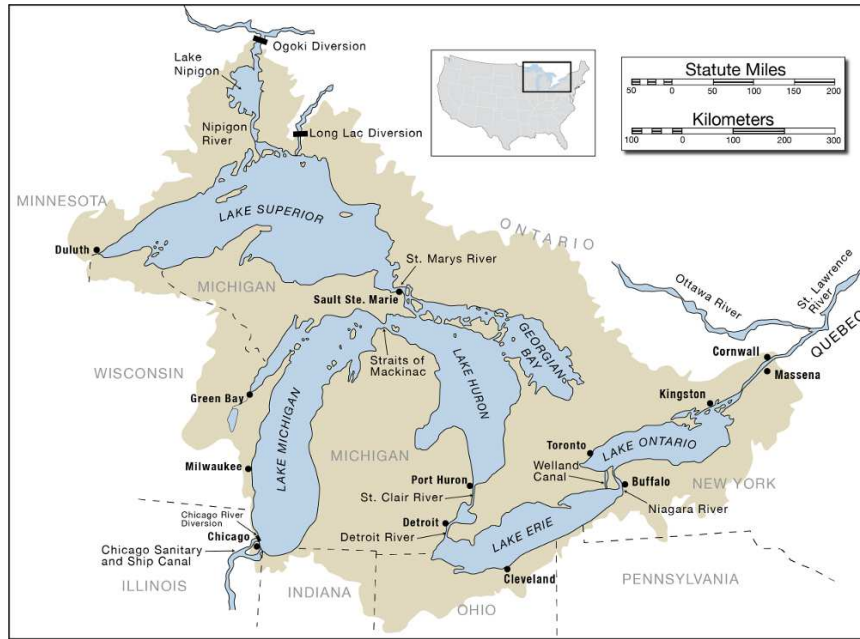
CONTACT J. P. Smith. Tel.: +1-734-741-2252, Fax: +1 734-741-2055, Email: joeseph@umich.edu

Figure 1. The Laurentian Great Lakes and their basin (light brown region) including location of major cities, interbasin diversions, and connecting channels.

employed to understand hydrological systems in numerous practical applications including water resources management decision support, and guidance on policies for consumptive use and irrigation practices [77]. Within a WBM, the balance may be expressed as the flow through a primary river – otherwise known as a rainfall-runoff model [3, 54], the change in water elevation of a lake [39, 46], or the soil moisture content within an area of focus [18, 62]. Modeling at the scale of the large Laurentian Great Lakes (figure 1), of which Superior and Michigan-Huron are the focus in this publication, is challenging as the lakes under study may span multiple countries and data are sparse [71], both in terms of temporal density and spatial coverage.

Existing large lake WBMs typically perform additive accounting with minimal accounting of uncertainty. Some water balance components are described by a single source of data while others are described by a single, potentially biased method which generates estimates. Gibson et al. (2006) [28] developed an additive WBM of the Great Slave Lake (GSL) in Canada. The GSL WBM was calibrated on observed water levels and incoming streamflow estimates which they believed contained the greatest amount of uncertainty. Additionally, the GSL WBM incorporated a large measurement record of the outflows through the Mackenzie River, Thiessen weighted precipitation gauge estimates, and simulated evaporation. Additive WBMs have also been developed for Lake Tana and Lake Victoria. Utilizing 1) precipitation data from Bahr Dar Station near southern Lake Tana, 2) the Penman equation [57] for evaporation given net short-wave radiation data from Addis Ababa Geophysical Observatory, and 3) available river discharge data, Kebede et al. (2006) solved an additive water balance equation for Lake Tana using Microsoft Excel's (Redmond, Washington, USA) Solver utility [42]. Piper et al. (1986) [58] conducted a similar analysis of Lake Victoria, averaging 8 precipitation gauges around the lake, partially simulated inflows, and Penman evaporation estimates.

As an enhancement of the additive WBM, we developed a prototype large lake sta-

tistical water balance model (L2SWBM) [30], seeking an understanding of drivers in the 2013-2014 record-setting water level rise on Lakes Superior and Michigan-Huron [31], the two largest lakes on Earth by surface area [33]. We leveraged state-of-the-art software for Markov chain Monte Carlo (MCMC) simulation of Bayesian Networks to assimilate regional estimates of water balance components (see section 1.1), developing a first-of-its-kind model that incorporates measurement uncertainty, correlation, and bias [6, 43, 65, 66], while closing the water balances of the lakes. We recognize that Bayesian WBMs have been developed previously for rainfall-runoff models [5], including WBMs utilizing frameworks such as Generalized Likelihood Uncertainty Estimation (GLUE) and the Water And Snow Balance Modeling (WASMOD) system [11, 22, 23, 40]. Prior to our prototype, however, we did not know of other studies that developed a Bayesian WBM for large lakes incorporating multiple independent estimates of water balance components.

Additionally, in developing a prototype L2SWBM, we knew of limited, if any, methodological guidance for developing and selecting a suitable WBM in light of criteria relevant to water resource management agencies, policy makers, and other model end-users. A lack of guidance in L2SWBM development may have enabled development of a computationally expensive prototype. Our prototype Superior and Michigan-Huron L2SWBM described the lakes' water balances as cumulative sums of monthly changes in water level or height ($\Delta H_{l,t,C}$), a proxy for water storage, starting at a specified base month. For the prototype, the base month was January of 2005, with the period of study ending December 2014, for a total of T = 120 months. At each time step, t, the prototype model aggregated all components of the water balance of each lake, l, from the base month through t, conceptually following the continuous time, or long-term yield, model of the Soil and Water Assessment Tool (SWAT [4, 41]):

$$\Delta H_{l,t,C} = \sum_{i=1}^{t}(P_{l,i} - E_{l,i} + R_{l,i} + I_{l,i} - Q_{l,i} \pm D_{l,i} + \epsilon_{l,i}), t \in [1,T] \qquad (1)$$

where (all in mm over each lake surface area) ΔH is assumed to be the difference between water levels at the beginning of months 1 and $t+1$, P is over-lake precipitation, E is over-lake evaporation, R is lateral tributary runoff into the lake, I is inflow from an upstream connecting channel, Q is outflow to a downstream connecting channel, D represents diversions into or (expressed as a negative value) out of the lake basin, and ϵ is a process error [1] term accounting for thermal expansion, glacial isostatic rebound, groundwater fluxes, and other sources of variability in monthly water levels not explained by water balance components P, E, R, I, Q, and D alone, nor are consistently measured in terms of impact on water level. The prototype L2SWBM, according to results in this manuscript, can take roughly 16 hours to simulate the network and acquire reliable water balance component estimates.

While the prototype L2SWBM differentiated hydrologic drivers of the 2013-2014 water level rise on Lakes Superior and Michigan-Huron under a closed water balance [56] for the 120 months of analysis, regional water resource management authorities have expressed interest in an expanded version of the model applied to all of the Laurentian Great Lakes and across a longer historical period – about 65 years (or 780 months), compared to just 10 (or 120 months) for the prototype. Long run times hinder exploration and formal assessment of different model formulations, and a 16 hour run time is problematic considering that the prototype model only includes Lake Superior

and Lake Michigan-Huron for the 120 months between 2005 to 2014. Our need to explore different model formulations arises, in part, from water managers' comments that St. Clair River flows inferred from the prototype L2SWBM are biased with a broad, unrealistic range of uncertainty, and that future L2SWBM development should reflect stronger *a priori* opinions about the accuracy of *in situ* measurements in the St. Clair and other connecting rivers, or connecting channels [55, 60]. Prototype L2SWBM channel flow inference bias may reflect unresolved uncertainties in individual lake water balance component estimates, which may propagate and accumulate through the Laurentian Great Lakes hydrologic system as represented by Bayesian networks. In essence, our goal is to limit the amount of cumulative uncertainty from Lake Superior through Lake Ontario and the St. Lawrence River in an expanded version of the L2SWBM.

The objective of this study, therefore, is the development of a framework for systematic experimentation, evaluation, and selection of alternative formulations of an L2SWBM. In this manuscript, we applied the framework to the prototype L2SWBM for Lakes Superior and Michigan-Huron to demonstrate how it can be used to improve model efficiency while incorporating *a priori* opinions about biases and uncertainties in existing data sources for components of the Great Lakes hydrologic cycle. We expect the new framework will be useful to improve not just the Great Lakes L2SWBM, but also variations for other large lakes of the world, and that the resulting new Great Lakes L2SWBM, following implementation of our recommended improvements, will be suitable for deployment in operational environments and for expansion across the entire Great Lakes system over a longer historical period.

1.1. Data

We used monthly, 1-dimensional (depth over lake surface), time-series data from a variety of independent sources to develop and test the Great Lakes L2SWBM (table 1). Data are used specifically in deriving water balance component prior probability distributions and likelihood functions described in sections 2.2 and 2.3. Data sources include the National Oceanic and Atmospheric Administration's Great Lakes Environmental Research Laboratory (NOAA-GLERL), Environment and Climate Change Canada (ECCC), and the Coordinating Committee on Great Lakes Basic Hydraulic and Hydrologic Data (CCGLBHHD, hereafter referred to as the Coordinating Committee), an ad hoc group of science agencies from both the United States and Canada.

NOAA-GLERL has, for many years, developed the Great Lakes Monthly Hydrometeorological Database (GLM-HMD) [36]. The GLM-HMD utilizes a suite of models to generate 1-dimensional estimates of precipitation, evaporation, and runoff. GLM-HMD precipitation estimates are derived from Thiessen weighting of meteorological station precipitation estimates across the Great Lakes basin [16]. 1-dimensional estimates of evaporation in the GLM-HMD utilize regional meteorological measurements of wind speed, dew point, cloud cover, and temperature input into the Large Lake Thermodynamics model (LLTM, [14, 15, 38]). United States Geological Survey (USGS) and Water Survey Canada (WSC) streamflow estimates across the basin are aggregated into GLM-HMD estimates of runoff for each lake via a conventional Area-Ratio Method (ARM) [24]. Lastly, in addition to the ARM runoff model estimates, we utilized runoff estimates from the Large Basin Runoff Model (LBRM)[17], which simulates water movement in a watershed through two soil layers (upper and lower), groundwater deposits, and evaporation, using meteorological station temperature and precipitation

Variable	Data source	Year range used	Mean	Median	S.D.	2.5%	97.5%
$y_{SUP,\Delta H,t,1}$	CCGLBHHD [12]	2005-2014	0.19	-10	72.07	-110	150
$y_{SUP,\Delta H,t,12}$	CCGLBHHD [12]	2005-2014	-1.69	0	152.88	-300	320
$y_{SUP,\Delta H,t,C}$	CCGLBHHD [12]	2005-2014	NA	NA	NA	NA	NA
$y_{SUP,P,1,t}$	GLM-HMD [36]	1950-2014	65.53	61.65	28.13	21.60	128.05
$y_{SUP,P,2,t}$	CaPA [45]	2005-2014	75.27	74.32	28.26	29.00	134.57
$y_{SUP,E,1,t}$	GLM-HMD (LLTM) [36]	1950-2014	46.06	40.69	42.18	-4.96	128.79
$y_{SUP,E,2,t}$	GEM-MESH [19]	2005-2014	48.85	45.56	41.18	-7.74	122.08
$y_{SUP,R,1,t}$	GLM-HMD (ARM) [36]	1950-2014	47.07	37.63	27.20	18.24	119.33
$y_{SUP,R,2,t}$	NOAA-GLERL LBRM [17]	1950-2014	50.77	44.15	23.41	23.24	111.27
$y_{SUP,Q,1,t}$	CCGLBHHD [12]	1950-2014	69.71	66.44	16.67	47.65	108.38
$y_{SUP,Q,2,t}$	IGS [73]	Nov. 2008-2014	58.20	51.61	16.31	37.60	100.50
$y_{SUP,D,1,t}$	CCGLBHHD [12]	1950-2014	4.91	4.22	2.59	1.27	11.21
$y_{MHU,\Delta H,t,1}$	CCGLBHHD [12]	2005-2014	0.80	-10	72.65	-120	155.25
$y_{MHU,\Delta H,t,12}$	CCGLBHHD [12]	2005-2014	1.46	-20	250.49	-470	488
$y_{MHU,\Delta H,t,C}$	CCGLBHHD [12]	2005-2014	NA	NA	NA	NA	NA
$y_{MHU,P,1,t}$	GLM-HMD [36]	1950-2014	70.16	68.25	27.16	24.35	132.99
$y_{MHU,P,2,t}$	CaPA [45]	2005-2014	81.09	79.14	28.75	35.40	140.73
$y_{MHU,E,1,t}$	GLM-HMD (LLTM) [36]	1950-2014	42.68	35.12	37.36	-4.53	118.31
$y_{MHU,E,2,t}$	GEM-MESH [19]	2005-2014	63.18	61.53	44.47	0.93	146.12
$y_{MHU,R,1,t}$	GLM-HMD (ARM) [36]	1950-2014	60.73	53.1	31.81	22.22	137.90
$y_{MHU,R,2,t}$	NOAA-GLERL LBRM [17]	1950-2014	62.26	56.40	28.66	25.32	131.77
$y_{MHU,Q,1,t}$	CCGLBHHD [12]	1950-2014	119.77	119.42	14.26	90.39	144.42
$y_{MHU,Q,2,t}$	IGS [73]	Nov. 2008-2014	112.19	113.74	10.11	86.13	128.42
$y_{MHU,D,1,t}$	CCGLBHHD [12]	1950-2014	2.05	2.02	0.56	1.16	3.22

Table 1. Summary of data sets used to develop water balance component prior probability distributions and as a basis for likelihood functions. Units for statistics – mean, median, standard deviation (S.D.), 2.5% and 97.5% quantiles – are millimeters over the respective lake surface. Unless otherwise specified, year range specified for each data set indicates availability from January of the first year through December of the second year. See table 2 for definitions of variables in the first column.

measurements as inputs.

Additional 1-dimensional, over-lake precipitation estimates are derived from gridded outputs of Environment and Climate Change Canada's (ECCC) version of the Canadian Precipitation Analysis (CaPA). CaPA utilizes short-term numerical weather prediction (NWP) models, along with meteorological station precipitation estimates from a collection of networks across Canada and the United States. NWP models depend on the Global Environmental Multiscale (GEM) model, which along with the Modélisation Environmentale - Surface et Hydrologie's (MESH) surface model, produce additional evaporation estimates utilized in this paper [19, 45].

The Coordinating Committee produces daily surface water elevation, or water level estimates, which we used to compute observations of ΔH. Water levels for the Laurentian Great Lakes are estimated via a series of water level gauges around the coasts maintained by NOAA National Ocean Service's Center for Operational Oceanographic Products and Services (NOAA/NOS CO-OPS) and the Canadian Department of Fisheries and Oceans' Canadian Hydrographic Service (DFO-CHS). To adjust for geological phenomena such as isostatic rebound, or the continued expansion of the Earth's crust from glacial retreat, water level estimates reference the International Great Lakes Datum (IGLD).

Additionally, the Coordinating Committee has historically developed connecting channel and diversion flow estimates within the Great Lakes basin. Connecting channel flows are estimated using a variety of methods, depending on the physical environment at the outlet of each lake. Flow estimates for the St. Marys river connecting Lakes Superior and Michigan-Huron, for example, are computed from the flows through a collection of dams and marine navigation locks between Sault Ste. Marie, Michigan in the United States, and Sault Ste. Marie, Ontario, Canada. For the St. Clair River, a combination of Acoustic Doppler Velocity Meter (ADVM) measurements and stage-fall discharge equation estimates produce the time-series data implemented in the L2SWBM. As a second source of channel flow estimates, ADVMs are used within International Gauging Stations (IGS). IGS used in this study are located at Sault Ste. Marie (for outflows from Lake Superior) and Port Huron (for outflows from Lake Michigan-Huron) and are maintained through a partnership between the USGS and WSC.

Measurements of diversions into (or out of) each lake basin include the Ogoki River and Long-Lac diversions into Lake Superior, and the Chicago River diversion out of Lake Michigan-Huron. We assumed that channel flows and diversions make their contribution to the water balance of a lake at the lake's outlet, downstream lake's inlet, or the point where a diversion enters or exits a lake. A notable challenge to this assumption includes the Ogoki diversion. Water diverted from the Ogoki River must first pass through Lake Nipigon (northern-most lake in figure 1) before it arrives in Lake Superior, thus there is an unknown amount of residence time before the water is actualized in the Lake Superior balance. As the diversion is small compared to other components of the water balance, however, we assume the impact uncertainty has on the water balance is minimal.

For further reading on coordinated estimates of water level, channel flows, and diversions, see [30].

6

Symbol	Description
Subscripts and related variables	
t	An individual month, spans $[1, T]$
T	Total months in analysis, 120 from January 2005 through December 2014 in this manuscript
$c(t)$	Calendar month $[1, 12]$ that month t is in
w	Rolling window for water balance analysis
j	Start month for an individual water balance window spanning $[1, T - w + 1]$
n	Independent estimate of θ
l	An individual lake, either SUP (Superior) or MHU (Michigan-Huron) in this manuscript
True, but unobserved parameters (mm over lake surface)	
$\Delta H_{l,j,w}$	Change in water level for lake l from beginning of month j to beginning of month $j + w$
$\Delta H_{l,t,C}$	Change in water level for lake l from beginning of month 1 to beginning of month t
$P_{l,t}$	Precipitation (total) over lake l in month t
$E_{l,t}$	Evaporation (total) from lake l in month t
$R_{l,t}$	Basin runoff (total) into lake l in month t
$I_{l,t}$	Connecting channel inflow (total) for lake l in month t
$Q_{l,t}$	Connecting channel outflow (total) for lake l in month t
$D_{l,t}$	Diversion from or to a lake (total) for lake l in month t
θ	Used to represent $P, E, R, Q,$ and D
Observed variables for likelihoods (mm over lake surface)	
$y_{l,H,t}$	Water level estimate for lake l at beginning of month t
$y_{l,\Delta H,j,w}$	Coordinated estimate of $\Delta H_{l,j,w}$
$y_{l,\Delta H,t,C}$	Coordinated estimate of $\Delta H_{l,j,C}$
$y_{l,\theta,n,t}$	n_{th} Independent estimate of $\theta_{l,t}$
Water balance component prior distribution parameters	
$\hat{\mu}_{l,E,c(t)}, \hat{\mu}_{l,Q,c(t)}, \hat{\mu}_{l,D,c(t)}$	Mean of historical data for E, Q, and D by calendar month $c(t)$ and lake l
$\hat{\mu}_{l,ln(R),c(t)}$	Mean of natural logarithm of historical data for R by calendar month $c(t)$ and lake l
$\hat{\tau}_{l,E,c(t)}, \hat{\tau}_{l,Q,c(t)}, \hat{\tau}_{l,D,c(t)}$	Precision of historical data for E, Q, and D by calendar month $c(t)$ and lake l
$\hat{\tau}_{l,ln(R),c(t)}$	Precision of natural logarithm of historical data for R by calendar month $c(t)$ and lake l
$\psi_{1,l,c(t)}, \psi_{2,l,c(t)}$	Shape and rate parameters for the prior distribution for P by calendar month $c(t)$ and lake l
Hyperparameters	
$\tau_{l,\theta,n}$	Precision of $y_{l,\theta,n,t}$ for all t
$\tau_{l,\Delta H,w}$	Precision of $y_{l,\Delta H,j,w}$ for all j
$\tau_{l,\Delta H,C}$	Precision of $y_{l,\Delta H,t,C}$ for all t
$\epsilon_{l,t}$	Process error in water balance equation for lake l in month t in mm over lake surface
$\epsilon_{l,c(t)}$	Seasonal process error by calendar month $c(t)$
$\tau_{l,\epsilon,c(t)}$	Seasonal precision of monthly process error by calendar month $c(t)$
$\eta_{l,\theta,n,t}$	Bias of $y_{l,\theta,n,t}$ in mm over lake surface
$\eta_{l,\theta,n,c(t)}$	Seasonal bias of $y_{l,\theta,n,t}$ by calendar month $c(t)$
$\tau_{l,\eta,c(t)}$	Seasonal precision of $y_{l,\theta,n,t}$ bias by calendar month $c(t)$
$\pi(...)$	Prior distribution for variable or parameter
τ	Precision $1/\sigma^2$, an expression of variance, σ^2, and standard deviation, σ

Table 2. Summary of variables and parameters employed in this manuscript

2. Methodology

Given the available data, we discuss the modeling frameworks, or Bayesian networks, we employed to infer values for each lake's water balance in this section. Further, we define a new water balance formulation designed to increase efficiency relative to the prototype L2SWBM. Lastly, we review parameter structures of the L2SWBM throughout this section, along with combinations of L2SWBM parameter structures that we tested in developing the model. For convenience, definitions of all variables and parameters in this section are in table 2.

2.1. Modeling framework

2.1.1. Encoding the Bayesian Network

With all variations of the L2SWBM, we inferred values for each component of each lake's monthly water balance, along with the other model parameters (e.g. process error described in section 2.2), through statistical models known as Bayesian networks [20, 50]. We programmed the Bayesian networks in the BUGS modeling language (Bayesian inference Using Gibbs Sampling [47, 48]), describing prior distributions, likelihoods, and posterior predictive distributions highlighted in all of section 2. For other examples of BUGS applications, see Armero et al. (2008) [2] and Blangiardo and Baio (2014) [7]. To compile and sample the complete likelihood function, joint, and conditional posterior distributions of the Bayesian Networks, we used JAGS [Just Another Gibbs Sampler; see 59], and the 'rjags' package in the R statistical software environment [61]. JAGS, despite what its name implies, utilizes a variety of samplers, and for our models, JAGS utilized Gibbs and slice samplers. Slice samplers are used on distributions describing non-negative, asymmetrically distributed variables, being precipitation and runoff (see section 2.3.1).

2.2. Water balance

For our new, experimental L2SWBMs, instead of a cumulative water balance (equation 1), we programmed a formulation in which changes in lake storage on lake l are considered across a period of w months. $\Delta H_{l,j,w}$ is defined as the difference between the lakewide-average surface water elevation at the beginning of month j, and the lakewide-average surface water elevation at the beginning of month $j + w$ (we hereafter refer to w as the length, in months, of the water balance rolling window). Changes in lake storage are then related to monthly-total water balance components as follows:

$$\Delta H_{l,j,w} = H_{l,j+w} - H_{l,j} = \sum_{i=j}^{j+w-1} \left(P_{l,i} - E_{l,i} + R_{l,i} + I_{l,i} - Q_{l,i} + D_{l,i} + \epsilon_{l,i} \right) \quad (2)$$

We note $I_{SUP,t} = 0$ because Lake Superior is the most upstream of the Laurentian Great Lakes and there is no inflow from a connecting channel. $I_{MHU,t} = 0.7(Q_{SUP,t})$, where 0.7 is a scaling factor accounting for the difference between surface areas of the two lakes. Through $Q_{SUP,t}$ and $I_{MHU,t}$, we linked the lakes in the model and ensured consistent inferences of flows through the St. Marys river.

Observations $y_{l,\Delta H,t,w}$ were computed from coordinated beginning of month estimates, and linked to the true value $\Delta H_{l,j,w}$ (equation 2) via the likelihood:

$$y_{l,H,j+w} - y_{l,H,j} = y_{l,\Delta H,j,w} \quad \sim \quad \mathsf{N}(\Delta H_{l,j,w}, \tau_{l,\Delta H,w}) \tag{3}$$

where precision $\tau_{l,\Delta H,w}$ is given a vague $\mathsf{Gamma}(0.01, 0.01)$ prior. No variations of this formulation were considered.

We recognize identifiability [21, 29, 63, 64] is a challenge with the additive balance in equation 2 being a part of the L2SWBM. In fact, the challenge of identifiability in WBMs was indirectly highlighted by Piper et al. (1986) [58], who noted that "it is not possible to distinguish easily between underestimates of rainfall and over-estimates of evaporation". By analyzing convergence of our experimental L2SWBMs (elaborated upon in section 2.4.1), we discover identifiable models, even though defining identifiability is difficult in a Bayesian context, where inferences are best given a model and data, not just a model [25]. The odds of finding an identifiable model are thus increased given strong prior distributions for the components θ, component estimates' biases η, and process error ϵ (described later in this section), along with prior distributions for estimates' precisions τ that grant more weight to other parameters of the network. Prior specifications for θ, η, and τ are described in section 2.3.

In discovering an identifiable L2SWBM, we compared three sets of models in the experiment design detailed in section 2.4, where each set has a different water balance formulation. The first set uses the balance computation in equation 1 as a basis of comparison. Observations of change in storage in the first set of models are denoted $y_{l,\Delta H,t,C}$ in table 1, where C indicates a cumulative water balance over the analysis period. Further, $\Delta H_{l,t,C} = H_{l,t+1} - H_{l,1}$, i spans $[1, t]$ in the summation in equation 2, and $y_{l,H,t+1} - y_{l,H,1} = y_{l,\Delta H,t,C}$ for equation 3. The other two sets of experimental models with respect to water balance formulation use equation 2 with rolling windows of $w = 1$ and $w = 12$ months. We not only intend to demonstrate a reduction in model computation time with the latter two sets in contrast to the first, but also assess the impact of different rolling window lengths on water balance estimates (e.g. monthly, seasonal, and inter-annual scales) relevant to regional water resource management decisions.

2.2.1. Process error

Additionally, we considered three alternative structures for process error $\epsilon_{l,t}$. The first, and simplest, is where we assume $\epsilon_{l,t} = 0$ as in the prototype model's implementation and unexplained variability in observed changes in storage propagates into water level measurement uncertainty (equation 3) and the uncertainty of other water balance components (see section 2.3). The second structure for process error strictly tracks potential seasonal variation, mapping each $\epsilon_{l,t}$ to one of twelve 'fixed', calendar-month $c(t)$ specific terms such that:

$$\begin{aligned} \epsilon_{l,t} &= \epsilon_{l,c(t)} \\ \pi(\epsilon_{l,c(t)}) &\sim \mathsf{N}(0, 0.01) \end{aligned} \tag{4}$$

where variance ($\sigma^2 = 100$) is expressed in terms of precision ($\tau = 1/\sigma^2 = 0.01$) in the vague, zero-mean prior. The third and final alternative structure for process error

is hierarchical, where each $\epsilon_{l,t}$ is given a vague prior. For each monthly process error prior, the mean is mapped to a calendar-month-specific term as in equation 4, while the precision is also calendar-month-specific, with all twelve precisions given a vague prior:

$$
\begin{aligned}
\pi(\epsilon_{l,t}) &\sim \mathsf{N}(\epsilon_{l,c(t)}, \tau_{l,\epsilon,c(t)}) \\
\pi(\epsilon_{l,c(t)}) &\sim \mathsf{N}(0, 0.01) \\
\pi(\tau_{l,\epsilon,c(t)}) &\sim \mathsf{Gamma}(0.05, 0.05)
\end{aligned}
\tag{5}
$$

Alternative structures for ϵ represented in equations 4 and 5 are intended to isolate water level measurement uncertainty from uncertainty in the balance model. We therefor modeled ϵ at seasonal and monthly temporal resolutions, respectively, while $\tau_{l,\Delta H,w}$ (equation 3) is assumed to be constant throughout the analysis period.

2.3. Water balance component (θ) priors and likelihoods

We treat water balance components ($\theta \in [P, E, R, Q, D]$) as random variables in the L2SWBM, attributing informative prior distributions and likelihoods, the latter of which we link input independent estimates. In this sub-section we first describe the prior distributions we develop, and then the likelihoods.

2.3.1. Prior distributions

For water balance component prior distributions ($\pi(\theta_{l,t})$), we fitted probability density functions to historical monthly data, aggregated by the 12 calendar months (sample of distributions shown in figure 2). To calculate prior distribution parameters, we used data for the period 1950 thru 2004 from the GLM-HMD and coordinated data sets – consistently available data from before the analysis period of 2005-2014. While we could have used less informative priors, we believe it would have been indefensible to use vague or non-informative priors given available data and expert hydrological knowledge.

True values of evaporation (E), channel flow (Q), and diversion (D) variables were given normal prior distributions:

$$
\begin{aligned}
\pi(E_{l,t}) &\sim \mathsf{N}(\hat{\mu}_{l,E,c(t)}, 0.5\hat{\tau}_{l,E,c(t)}) \\
\pi(Q_{l,t}) &\sim \mathsf{N}(\hat{\mu}_{l,Q,c(t)}, 0.5\hat{\tau}_{l,Q,c(t)}) \\
\pi(D_{l,t}) &\sim \mathsf{N}(\hat{\mu}_{l,D,c(t)}, \hat{\tau}_{l,D,c(t)})
\end{aligned}
\qquad
\begin{aligned}
&(6) \\
&(7) \\
&(8)
\end{aligned}
$$

with means ($\hat{\mu}_{l,*,c(t)}$) and precisions ($\hat{\tau}_{l,*,c(t)}$) calculated from the historical data. Because the range of historical values of evaporation and channel outflows is quite narrow for the late spring and early summer months of the year, we halved the calculated precisions of the prior probability distributions for evaporation and channel outflows to accommodate factors such as climate change [52]. We do not expect empirically-derived prior probability distributions for other, more intrinsically variable water balance components to restrict the estimation of their respective posterior probability distributions.
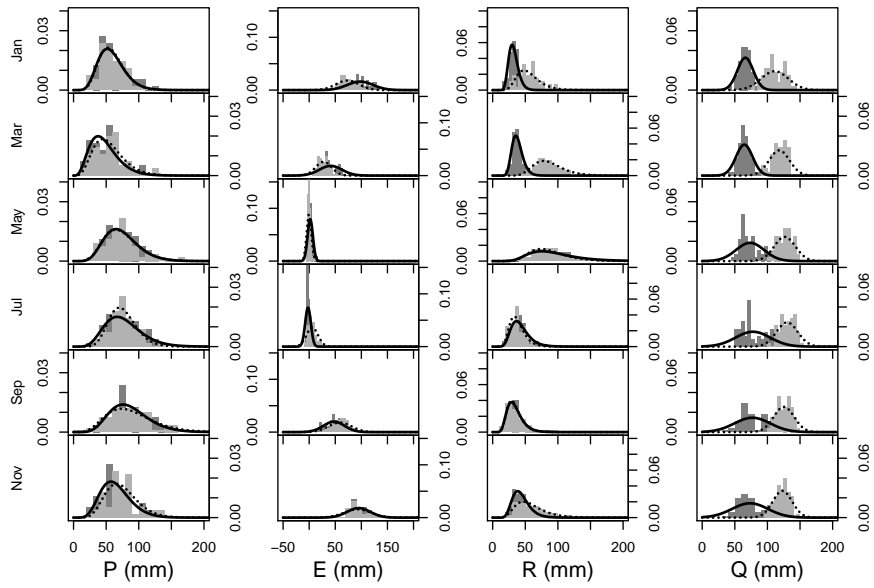
10

Figure 2. Sample of prior distributions for all θ, except diversions (D), for every other month starting with January and ending with November. We constructed prior distributions in such a way to capture seasonal variability, if any, across components. Histograms represent the available historical data supporting the fitted prior distributions while the lines represent the fitted density functions. Dark gray histogram bars with solid black density fit lines represent Lake Superior's priors, and light gray bars with dotted density fit lines represent Lake Michigan-Huron's priors.

For the true values of non-negative components precipitation and runoff, we fitted, respectively, Gamma [37] and log-normal prior distributions:

$$\pi(P_{l,t}) \sim \mathsf{Gamma}(\psi_{1,l,c(t)}, \psi_{2,l,c(t)}) \tag{9}$$

$$\pi(R_{l,t}) \sim \mathsf{ln\ N}(\hat{\mu}_{l,ln(R),c(t)}, \hat{\tau}_{l,ln(R),c(t)}) \tag{10}$$

For runoff, we calculated the means $(\hat{\mu}_{l,ln(R),c(t)})$ and precisions $(\hat{\tau}_{l,ln(R),c(t)})$ for the prior distributions with the natural logarithms of the historical data. Gamma distributions for precipitation require non-trivial maximum likelihood shape $(\psi_{1,l,c(t)}$, equation 11) and rate $(\psi_{2,l,c(t)}$, equation 12) parameters (per Thom (1958) [72]) which we calculated from the historical data such that:

$$\psi_{1,l,c(t)} = \frac{1}{4\phi_{l,c(t)}}\left(1 + \sqrt{1 + \frac{4\phi_{l,c(t)}}{3}}\right) \tag{11}$$

$$\phi_{l,c(t)} = \ln(\hat{\mu}_{l,P,c(t)}) - \hat{\mu}_{l,ln(P),c(t)}$$

$$\psi_{2,l,c(t)} = \psi_1/\hat{\mu}_{l,P,c(t)} \tag{12}$$

where $\hat{\mu}_{l,P,c(t)}$ and $\hat{\mu}_{l,ln(P),c(t)}$ are the means of the historical precipitation observations for a given calendar month $c(t)$ and natural logarithms thereof, respectively. While channel flow and diversion values are generally non-negative over the course of a calendar month, we believe inferences of channel flows and diversions will not be negative, and that any negative inferences of diversions will be negligible given their scale compared to other water balance components.

We included in supplementary material for this manuscript histograms of all seasonal historical data for each water balance component and each lake, along with the fitted prior distributions. No variations in $\pi(\theta_{l,t})$ formulations are examined for this manuscript.

2.3.2. Likelihoods

We linked the water balance and independent estimates of water balance components via normal distributions. Incorporating our beliefs of a data source's potential bias, we established for lake l a relationship between the observed value of a component θ from data source n on month t $(y_{l,\theta,n,t})$ to the true value of $\theta_{l,t}$ via the likelihood:

$$y_{l,\theta,n,t} \sim \mathsf{N}(\theta_{l,t} + \eta_{l,\theta,n,t}, \tau_{l,\theta,n}), \theta \in [P, E, R, Q, D] \tag{13}$$

with $\eta_{l,\theta,n,t}$ representing observation bias, and component likelihood precision $\tau_{l,\theta,n}$ given a vague $\mathsf{Gamma}(0.1, 0.1)$ prior. For non-negative variables precipitation and runoff, we assumed that the non-negative, asymmetric priors we applied will ensure non-negative inferences of the components' true values, despite the application of symmetric and potentially negative normal likelihoods.

We formally considered two alternative structures for bias $\eta_{l,\theta,n,t}$ of data sources $y_{l,\theta,n,t}$ (equation 13). Unlike process error (ϵ), we did not consider an alternative where $\eta_{l,\theta,n,t} = 0$, as we believe biases are inherent in independent water balance component

estimates, such as precipitation (see Holman et al. (2012), [35]). Thus, the first alternative for $\eta_{l,\theta,n,t}$ we used, following the structure of equation 4 and the prototype model's implementation, strictly tracks seasonal variation:

$$
\begin{aligned}
\eta_{l,\theta,n,t} &= \eta_{l,\theta,n,c(t)} \\
\pi(\eta_{l,\theta,n,c(t)}) &\sim \mathsf{N}(0, 0.01)
\end{aligned}
\tag{14}
$$

The second alternative structure for bias, following the structure of equation 5, is hierarchical:

$$
\begin{aligned}
\pi(\eta_{l,\theta,n,t}) &\sim \mathsf{N}(\eta_{l,\theta,n,c(t)}, \tau_{l,\eta,\theta,n,c(t)}) \\
\pi(\eta_{l,\theta,n,c(t)}) &\sim \mathsf{N}(0, 0.01) \\
\pi(\tau_{l,\eta,\theta,n,c(t)}) &\sim \mathsf{Gamma}(0.05, 0.05)
\end{aligned}
\tag{15}
$$

Lastly, we reflected the *a priori* opinions of regional water resource management authorities regarding the accuracy of channel flow (Q) and diversion (D) estimates through similar bias constructions. Following informal protocols for soliciting *a priori* expert opinions [8, 74], we found that regional water management authorities believe that monthly channel flow data can depart from true channel flows by between roughly 180 and 270 cubic meters per second (cms) – 6 to 9mm of water over the surface of Lake Superior, and 4 to 6mm of water over the surface of Lake Michigan-Huron. Departure of diversion estimates from their true values, given their smaller magnitudes, are less (see table 1). In a theoretical 95% credible interval produced from the previously defined $\eta_{l,\theta,n,t}$ (equations 14 and 15), water balance component observations may depart from the true value of components by about 20 mm (precision = 0.01, standard deviation is thus 10), more than double the suggested departure of channel flow and diversion estimates.

Thus, for $\zeta \in (Q, D)$ in equations below, we modified equations 14 and 15, increasing the prior precision of the seasonal bias parameter ($\eta_{l,\zeta,n,c(t)}$). We recognize we could have done a more specific prior for each estimate of each channel flow or diversion. However, in the interest of minimizing experimental models to run and testing solely the impact of restricting bias on channel flow and diversion estimates, we applied a prior precision of 0.25 for the seasonal bias of all estimates of channel flows and diversions (standard deviation of 2 mm, maximum theoretical 95% credible interval departure of 4 mm), accounting for a second set of experiments in section 2.4. Equation 14 thus becomes:

$$
\begin{aligned}
\eta_{l,\zeta,n,t} &= \eta_{l,\zeta,n,c(t)} \\
\pi(\eta_{l,\zeta,n,c(t)}) &\sim \mathsf{N}(0, 0.25)
\end{aligned}
\tag{16}
$$

and equation 15 thus becomes:

$$
\begin{aligned}
\eta_{l,\zeta,n,t} &\sim \mathsf{N}(\eta_{l,\zeta,n,c(t)}, \tau_{l,\eta,\zeta,n,c(t)}) \\
\eta_{l,\zeta,n,c(t)} &\sim \mathsf{N}(0, 0.25) \\
\tau_{l,\eta,\zeta,n,c(t)} &\sim \mathsf{Gamma}(0.05, 0.05)
\end{aligned}
\tag{17}
$$

Structures of $\eta_{l,\theta,n,t}$ represented in equations 14, 15, 16, and 17 are intended to, like structures of ϵ (equations 4 and 5), isolate water balance component observation uncertainty from uncertainty in the water balance. We therefor modeled $\eta_{l,\theta,n,t}$ at seasonal and monthly temporal resolutions, respectively, while $\tau_{l,\theta,n}$ (equation 13) is assumed to be constant throughout the analysis period.

We recognize that we utilized three different Gamma distributions as prior distributions for precisions (τ), which expressed different beliefs in the variability of particular parameters. $\tau_{l,\Delta H,w}$ (equation 3) were given $\mathsf{Gamma}(0.01, 0.01)$ priors, which have their greatest densities towards the lower precision values, reflecting our desire for the model to explore a range of change in storage and water balance component values in producing a closed water balance. $\tau_{l,\theta,n}$ (equation 13) were given $\mathsf{Gamma}(0.1, 0.1)$ priors, and have higher densities for higher precision values to propagate uncertainty into component observation bias terms $\eta_{l,\theta,n,t}$. Lastly, $\tau_{l,\epsilon,c(t)}$, and $\tau_{l,\eta,\theta,n,c(t)}$ (equation 5 and 15 respectively) were given $\mathsf{Gamma}(0.05, 0.05)$ priors, expressing our belief that monthly process errors and observation biases may vary from an unobserved, seasonal cycle at a magnitude less than the variability of $y_{\Delta H,j,w}$ and more than the variability of $y_{l,\theta,n,t}$.

Inferences of τ and η are analyzed and discussed in section 4.2.

2.4. L2SWBM Variations

We formally analyzed combinations of L2SWBM parameter structures, or L2SWBM variations, detailed in sections 2.2 and 2.3 using a modified factorial experiment design [53]. Table 3 lists the 26 models we assessed, incorporating options laid out in sections 2.2 and 2.3. Only two L2SWBMs, PROT and fPROT (for prototype) used the balance computation in equation 1 due to computational expense, differing by the modification to the prior on channel flow and diversion bias detailed in equation 16. The prototype L2SWBMs may be compared directly to models (f)01NF and (f)12NF as while they utilize balance equation 2, all other experimental factors are the same as the prototype. The remaining 24 L2SWBMs vary by rolling window length (1 or 12 months), whether and how they modeled process error ('N'one, 'F'ixed, or 'H'ierarchical), how they modeled water balance component observation bias ('F'ixed or 'H'ierarchical), and whether or not they constrained inference of bias for channel flows and diversions (equation 16 or 17, indicated by prefix 'f' for the model ID in the left-most column).

We consider the prototype model, utilizing balance equation 1, to be computationally cost prohibitive for temporal and spatial expansion (across all Great Lakes). The number of calculations required per analysis time step in the prototype increases as the model iterates through the analysis period. For our non-prototype experimental models utilizing equation 2, however, the number of required calculations per time step is fixed.

2.4.1. Model evaluation

Experimentation is intended to find a robust L2SWBM formulation that adequately closes the water balance, comparable to the prototype, while doing so more efficiently. With our experiment design and 24 non-prototype L2SWBMs, we aimed to identify L2SWBM structures that better close the water balance and better converge [26] on true values for our parameters of interest. We also aimed to identify L2SWBM structures that should not be employed due to inadequate performance in terms of

Model ID	w	$\pi(\epsilon_{l,t})$	$\pi(\eta_{l,\theta,n,t})$	$\pi(\eta_{l,\zeta,n,t})$
PROT	C (eq. 1)	None	Fixed (eq. 14)	
01NF	1 (eq. 2)	(N)one	(F)ixed (eq. 14)	
01NH	1 (eq. 2)	(N)one	(H)ierarchical (eq. 15)	
01FF	1 (eq. 2)	(F)ixed (eq. 4)	(F)ixed (eq. 14)	
01FH	1 (eq. 2)	(F)ixed (eq. 4)	(H)ierarchical (eq. 15)	
01HF	1 (eq. 2)	(H)ierarchical (eq. 5)	(F)ixed (eq. 14)	
01HH	1 (eq. 2)	(H)ierarchical (eq. 5)	(H)ierarchical (eq. 15)	
12NF	12 (eq. 2)	(N)one	(F)ixed (eq. 14)	
12NH	12 (eq. 2)	(N)one	(H)ierarchical (eq. 15)	
12FF	12 (eq. 2)	(F)ixed (eq. 4)	(F)ixed (eq. 14)	
12FH	12 (eq. 2)	(F)ixed (eq. 4)	(H)ierarchical (eq. 15)	
12HF	12 (eq. 2)	(H)ierarchical (eq. 4)	(F)ixed (eq. 14)	
12HH	12 (eq. 2)	(H)ierarchical (eq. 4)	(H)ierarchical (eq. 15)	
fPROT	C (eq. 1)	None	Fixed (eq. 15)	(eq. 16)
f01NF	1 (eq. 2)	(N)one	(F)ixed (eq. 14)	(eq. 16)
f01NH	1 (eq. 2)	(N)one	(H)ierarchical (eq. 15)	(eq. 17)
f01FF	1 (eq. 2)	(F)ixed (eq. 4)	(F)ixed (eq. 14)	(eq. 16)
f01FH	1 (eq. 2)	(F)ixed (eq. 4)	(H)ierarchical (eq. 15)	(eq. 17)
f01HF	1 (eq. 2)	(H)ierarchical (eq. 4)	(F)ixed (eq. 14)	(eq. 16)
f01HH	1 (eq. 2)	(H)ierarchical (eq. 4)	(H)ierarchical (eq. 15	(eq. 17)
f12NF	12 (eq. 2)	(N)one	(F)ixed (eq. 14)	(eq. 16)
f12NH	12 (eq. 2)	(N)one	(H)ierarchical (eq. 15)	(eq. 17)
f12FF	12 (eq. 2)	(F)ixed (eq. 4)	(F)ixed (eq. 14)	(eq. 16)
f12FH	12 (eq. 2)	(F)ixed (eq. 4)	(H)ierarchical (eq. 15)	(eq. 17)
f12HF	12 (eq. 2)	(H)ierarchical (eq. 4)	(F)ixed (eq. 14)	(eq. 16)
f12HH	12 (eq. 2)	(H)ierarchical (eq. 4)	(H)ierarchical (eq. 15)	(eq. 17)

Table 3. Summary of our experimental design in which alternative models are configured with variations in the length of monthly water balance window (used in model inference) w, prior probability distributions for process error $\pi(\epsilon_{l,t})$, and prior probability distribution for data bias $\pi(\eta_{l,\theta,n,t})$. A window of C indicates the water balance of equation 1 was used in the model (see section 2.2).

balance closure or convergence. In fact, some of the proposed L2SWBM structures may be erroneous [11], and may be exposed through poor closure or convergence in comparison with other L2SWBMs. Water balance closure addresses a need in data to support water resource management decisions, while increased L2SWBM efficiency enables exploration of alternative L2SWBMs, which will be critical when we expand L2SWBMs to include the remaining Laurentian Great Lakes.

In analyzing water balance closure of the experimental L2SWBMs, we assessed closure across all 1, 12, and 60-month periods from 2005 through 2014, instead of closure through the entire 120 month period of study, which is less practical from an operational standpoint. Posterior predictive distributions [27, 44] simulate what observations of a variable could be given all other information in a model except the observations. We constructed the posterior predictive distributions for observations of change in storage such that:

$$\tilde{y}_{l,\Delta H,j,1} \quad \sim \quad \mathsf{N}(\Delta H_{l,j,1}, \tau_{l,\Delta H,w}) \tag{18}$$

$$\tilde{y}_{l,\Delta H,j,12} \quad \sim \quad \mathsf{N}(\Delta H_{l,j,12}, \tau_{l,\Delta H,w}) \tag{19}$$

$$\tilde{y}_{l,\Delta H,j,60} \quad \sim \quad \mathsf{N}(\Delta H_{l,j,60}, \tau_{l,\Delta H,w}) \tag{20}$$

where w is the rolling window used in an experimental L2SWBM. We used the same change in storage observation precision learned in the model to generate posterior predictive samples. Using MCMC samples from distributions 18, 19, and 20, we derived 95% credible intervals for, respectively, changes in storage across all 1, 12, and 60-month periods from 2005 through 2014. We then calculated the corresponding observed changes in storage: $y_{l,\Delta H,j,1}$, $y_{l,\Delta H,j,12}$, $y_{l,\Delta H,j,60}$. Hence, an experimental L2SWBM closes the water balance at a rate equal to the number of observations $(y_{l,\Delta H,j,1}$, $y_{l,\Delta H,j,12}$, $y_{l,\Delta H,j,60})$ that are within the 95% credible intervals of their respective posterior predictive distributions $(\tilde{y}_{l,\Delta H,j,1}$, $\tilde{y}_{l,\Delta H,j,12}$, $\tilde{y}_{l,\Delta H,j,60})$, divided by the respective number of observations (120, 109, and 61).

We recognize that our L2SWBM evaluation design (table 3) does not include water balance component inference using an L2SWBM with a rolling window (w) of 60 months and, furthermore, that a range of different rolling windows could have been explored for inference in our experiment design. Regardless, our approach addresses the question of whether water balance components inferred from an L2SWBM with only a 1-month rolling window (which may have the advantage of a relatively short computation time) close the water balance over periods longer than one month, or if a longer rolling window (in our case, assessed using a 12-month window) is needed.

For water balance closure assessment, we ran each L2SWBM alternative for $K = 250,000$ MCMC iterations across three parallel MCMC chains, and thinned the last 125,000 iterations of each chain (omitting the first 125,000 iterations as a 'burn-in' period) at even intervals such that the resulting chains each have 1,000 values. The resulting 3,000 MCMC samples for each parameter then serve as the basis for our posterior predictive water balance closure assessment, along with our posterior inferences of other parameters of interest (e.g. channel flows and diversions). We ran the L2SWBMs on a Windows 7 Professional (Microsoft, Redmond, WA, USA) workstation with a 64-bit Intel Core i7-3770 (3.4 GHz) processor with 32 GB of RAM. JAGS model code is included in the supplementary material.

Additionally, for each L2SWBM in our experimental design, we analyzed model convergence through $K = 250,0000$ MCMC iterations by calculating the potential scale

reduction factor (PSRF), also referred to as the Gelman-Rubin convergence statistic or $\hat{R}$ [26], every 10,000 iterations for all L2SWBM parameters. We, again, at every 10,000 iterations, treated half of the samples of each chain as burn-in, and thinned the latter half of each chain down to 1,000 samples. We calculated the PSRF using the `gelman.diag` function in the R package 'CODA' which returned both the median ($\hat{R}_{50}$) and 97.5% quantile ($\hat{R}_{97.5}$) of the PSRF. We assessed convergence by testing whether $\hat{R}_{50}$ and $\hat{R}_{97.5}$ approached (or decreased below) 1.1, per guidance from Gelman and Rubin (1992), with additional MCMC iterations. Parallel to assessing L2SWBM efficiency in terms of iterations required for convergence, we recorded the total time required for each L2SWBM to generate $K = 250,000$ MCMC iterations. The L2SWBM runs we executed for monitoring computation time did not include calculations for posterior predictive distributions because they serve as a basis for model verification only and would not, we believe, be encoded in a future version employed in routine operations.

In concluding L2SWBM comparison, we calculated the Deviance Information Criteria (DIC, [70]), as an MCMC-friendly substitute for the Akaike information criteria (AIC) and Bayesian information criteria (BIC). We drew 1000 samples via the `dic.samples` function in the R package 'CODA' using the 'pD' penalty type and calculated a mean score for each L2SWBM in our experimental design. We then compared the scores to the other tests we perform.

3. Application of Methodology

3.1. Analysis of water balance closure

Our analysis of 95% posterior predictive intervals for simulated changes in lake storage across 1, 12, and 60-month periods (table 4) indicates that most L2SWBMs conditioned on changes in storage across a 1-month window close the water balance for Lakes Superior and Michigan-Huron in simulations over a 1-month period, but do not effectively close the water balance in simulations over 12 and 60-month periods. Water balance component estimates conditioned on a rolling 12-month storage window, however, close the water balance for 12- and 60-month periods for Lakes Superior and Michigan-Huron, and come close to closing the water balance for both lakes on a 1-month storage window. For example, 95% posterior predictive intervals for monthly changes in storage derived from 12-month rolling window models included between 91% and 100% of the observed monthly changes in storage for Lake Superior, and between 79% and 98% of observed monthly changes in storage for Lake Michigan-Huron. Similarly, 95% posterior predictive intervals for 12- and 60-month changes in storage derived from 12- month rolling window models contained 97% to 100% of the observed monthly changes in storage for both Lakes Superior and Michigan-Huron.

Our results show slight improvements in balance closure occur through either a) the introduction alone of an explicit process error term or b) the relaxation of prior probability distributions for the bias of data sources via the introduction of a hierarchical structure. Applying a reduced range of bias in channel flow measurements yielded mixed results in terms of improving balance closure in an L2SWBM. L2SWBMs that inferred changes in storage over a 1-month window exhibited little impact on 1-month window closure rates post-application, in contrast to a maximum 17% drop (01NH to f01NH) post-application for 12 and 60 month closure rates. 12-month rolling window models were more robust, with the only decreases in performance occurring with 1-month changes in storage on Michigan-Huron — the percentage of observed changes

	Simulation with rolling window (months) of:											
	1		12		60			1		12		60	
Model	SUP	MHU	SUP	MHU	SUP	MHU	Model	SUP	MHU	SUP	MHU	SUP	MHU
NULL	98	98	99	100	100	100	fNULL	98	98	99	100	100	98
01NF	97	99	27	29	21	15	f01NF	98	98	24	17	13	7
01NH	98	100	35	38	21	23	f01NH	98	99	29	21	13	13
01FF	97	99	28	50	25	26	f01FF	98	99	28	39	23	23
01FH	99	100	39	52	25	34	f01FH	99	100	35	50	21	30
01HF	100	100	51	79	30	38	f01HF	100	100	45	75	25	36
01HH	100	100	55	74	41	38	f01HH	100	100	50	76	28	38
12NF	92	85	99	100	100	97	f12NF	91	79	100	100	100	97
12NH	95	84	100	100	100	100	f12NH	95	79	100	100	100	98
12FF	98	88	99	100	100	97	f12FF	98	86	99	100	100	97
12FH	98	92	100	100	100	100	f12FH	98	88	100	100	100	100
12HF	93	92	100	100	100	100	f12HF	95	88	100	100	100	100
12HH	98	98	100	100	100	100	f12HH	100	87	100	100	100	100

Table 4. Percent (%) of observed changes in lake storage within 95% posterior predictive intervals of model-simulated changes in storage across 1, 12, and 60 month periods for Lakes Superior (SUP) and Michigan-Huron (MHU) across all experimental models.

in lake storage within 95% posterior predictive credible intervals dropped between 2% and 11% after application.

A visual inspection of a representative time series (from the f01FF and f12FF models) comparing observed and simulated changes in storage over 1, 12, and 60-month periods (figure 3) underscores the degradation in skill when water balance components inferred from an 1-month window L2SWBM are used to simulate changes in lake storage across longer time periods. The visual inspection of the representative time series also indicates that while the percentage of observations within the 95% posterior predictive interval for the f12FF model (right column, figure 3) exceeds 95% when used to simulate 12- and 60-month cumulative changes in storage, overdispersion does not appear to be a significant problem. L2SWBMs that infer over narrower windows allow more freedom in the exploration of values for components in a given month. Due to a lack of information from other months, however, it is difficult to close the balance over longer time periods with those models. Larger windows for inference, however, shrink the range of possible values of water balance components, as the values must close a larger number of w month balance periods.

3.2. Model convergence and computation time

Results of our convergence analysis (figure 4) indicate that most experimental L2SWBMs approached convergence within 250,000 iterations, but that at least one of the several hundred parameters (up to 4,350 parameters) in each of our experimental L2SWBMs (represented by the maximum PSRF) did not fully converge. We found, for under half the models, just two or tree of the parameters in each model have a PSRF above 1.1. Models with a hierarchical data source bias structure, or a combination of 1) a 12-month rolling window for inference of changes in storage and 2) hierarchical process error and bias structure, had significantly more than three parameters not converge. We found it most common, with L2SWBMs that nearly converged completely, for two or three of the water balance component observation precision(s) $\tau_{l,\eta,\theta,n,c(t)}$ to be the parameter(s) that did not converge. For further reading on analyzing the
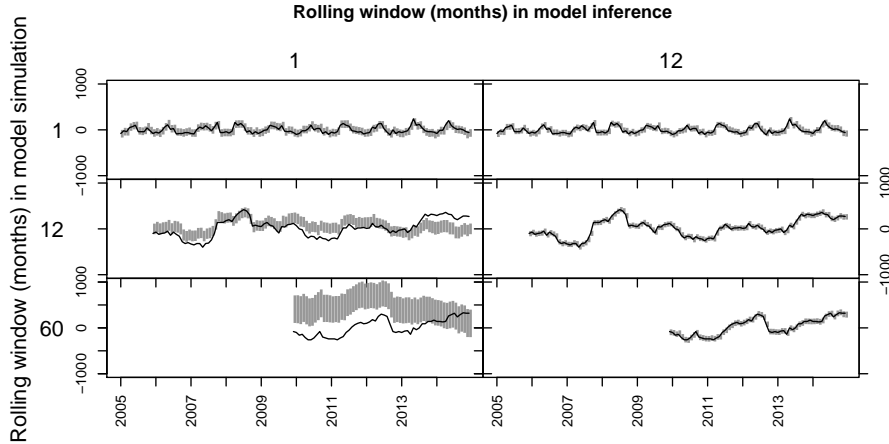
18

Figure 3. Comparison between observed (black line) and simulated (95% posterior predictive intervals; grey regions) changes in lake storage (mm over lake surface) across a period of 1, 12, and 60 months (indicated adjacent to left-hand vertical axes) for Lake Superior. Simulated changes are based on water balance components inferred using either a 1-month (left column) or 12-month (right column) window. Simulation results shown are based on the f01FF and f12FF models (per table 4). We note that models with a 1-month balance window do not adequately simulate long-term changes in storage, indicated by the black line falling outside of the gray regions plotted for those models and simulation windows. Visual comparison for Lake Michigan-Huron is omitted due to redundancy.

convergence of a model with many variables, see Brooks and Gelman (1998)[10]. We omit a figure illustrating convergence of models without informative prior probability distributions on channel flow and diversion estimate bias as the results are redundant.

We also find that the time to run an L2SWBM (to 250,000 iterations) with a 12-month rolling inference window (also figure 4) is roughly 14 hours less than the time required for the prototype L2SWBM, but roughly three times longer than the time to run a model with a 1-month inference window. The time required to run L2SWBMs with different process error structures are about equal, while implementing a hierarchical structure for data source bias adds up to 10 minutes compared with a fixed structure. These run times are dependent on the technical specifications of the computer used, as well as other applications being run simultaneously on the same computer. Run times will, therefore, likely differ across different computational environments.

3.3. DIC results

Table 5 shows the DIC scores for our experimental L2SWBMs. Model f12HH is favored over the rest of the experimental L2SWBMs based on the presented DIC scores. Interestingly, the two L2SWBMs that converge well and satisfactorily close the water balance – (f)12NF and (f)12FF – received comparable scores to the (f)PROT models, with only f12NF receiving a slightly worse score. We note that the DIC scores shown exhibit how DIC are not invariant to reparameterization [69]. In fact, a change in L2SWBM structure results in roughly a 1,000 to 4,000 DIC point difference.
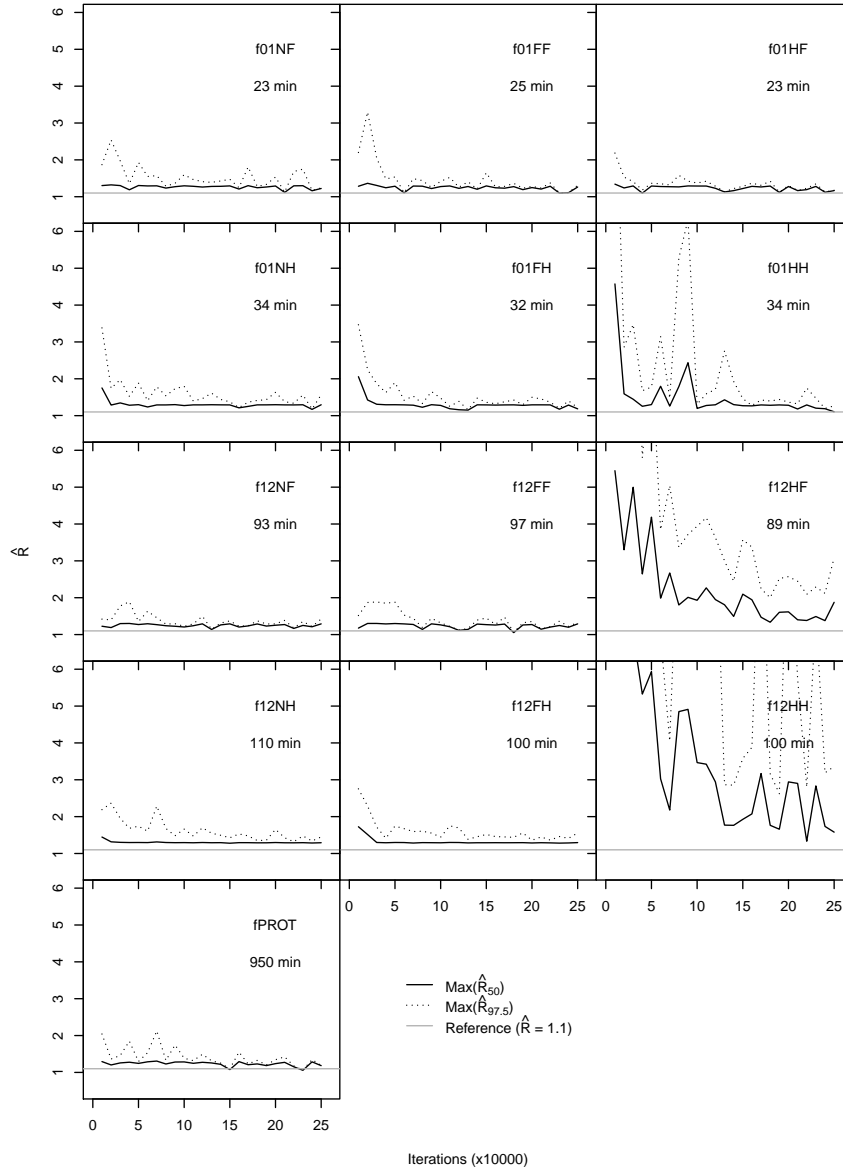
Figure 4. Evolution of the maximum value of convergence statistics $\hat{R}_{50}$ and $\hat{R}_{97.5}$ (from all parameters in a given model) across JAGS sampling iterations for L2SWBMs with informative prior probability distributions on channel flow and diversion estimate bias. Run times are beneath the L2SWBM label in each panel. We omit figures illustrating convergence of L2SWBMs without informative prior probability distributions on channel flow and diversion estimate bias as those results are redundant.

Model	DIC	Model	DIC	Model	DIC	Model	DIC
PROT	12665.06	fPROT	12649.40				
01NF	11992.45	f01NF	12142.76	12NF	12582.83	f12NF	12733.59
01NH	10271.64	f01NH	10031.27	12NH	10831.3	f12NH	10595.51
01FF	12347.55	f01FF	12118.43	12FF	12558.21	f12FF	12507.05
01FH	9870.43	f01FH	9814.96	12FH	10622.67	f12FH	10579.13
01HF	12323.85	f01HF	12031.26	12HF	10824.23	f12HF	11221.91
01HH	10124.29	f01HH	10263.95	12HH	9143.96	f12HH	8237.85

Table 5. DIC scores for our experimental L2SWBMs using the pD penalty.

3.4. Incorporating expert opinions on channel flow bias

Reducing the *a priori* range of potential bias in channel flow measurements significantly reduced the uncertainty and central tendency of our inferred channel flow estimates (figure 5) relative to the prototype model without significantly impacting variability and bias in the other inferred water balance components (table 6). For example, we find that uncertainty, or the standard deviation, in a sample of inferred posterior distributions for precipitation, evaporation, and runoff increased by no more than 2 mm from the prototype model to the f12FF and f12NF models.

4. Conclusion and Discussion

4.1. L2SWBM selection

Our experiment indicates that month-to-month water balance inference, or inference using only a one month rolling window, does not close the balance over time periods of 12 months or greater. As also exposed through our experiment design, MCMC convergence is greatly hindered, if not prevented, given a more complex hierarchical process error or component observation bias structure. DIC scores favored the more complex, non-convergent L2SWBMs, but we believe that is an artifact of DIC's sensitivity to reparameterization. Therefore, two model options can be recommended: f12NF and f12FF. Both options have a 12-month rolling water balance window, a fixed data source bias structure as in the prototype model, and constrained priors on bias for channel flow and diversion estimates. Whether or not process error is explicitly estimated on a seasonal basis is the difference between the two options, where the advantage in the former, or f12FF, is 7% more months with a closed water balance on a monthly basis. Additionally, both models required roughly 1.5 hours to compute 250,000 MCMC iterations – compared to 16 hours for the prototype model – and closed the water balance at a rate comparable to the prototype model over 1, 12, and 60 month periods, incorporating current opinions of regional water management authorities. These results give water resource managers and analysts flexibility in choosing to estimate process error, which may estimate the collective impact of groundwater fluxes, isostatic rebound, thermal expansion, and other unmeasured phenomena.

4.2. Impact of vague priors on posterior inferences of bias and precision

We found that vague Gamma$(0.01, 0.01)$ and Gamma$(0.1, 0.1)$ priors we applied for the precision of observed changes in storage $(\tau_{l,\Delta H,w})$ and independent water bal-

Parameter	PROT				f12NF				f12FF			
	Mean	S.D.	2.5%	97.5%	Mean	S.D.	2.5%	97.5%	Mean	S.D.	2.5%	97.5%
$P_{SUP,10}$	121.04	7.68	106.52	136.33	119.77	8.35	103.41	136.10	124.91	8.40	109.03	141.89
$E_{SUP,10}$	69.52	5.98	57.92	81.27	70.32	6.11	58.55	82.17	66.69	6.18	54.76	78.52
$R_{SUP,10}$	50.52	4.73	41.29	60.57	50.30	5.29	40.15	60.68	52.04	5.09	42.06	62.26
$Q_{SUP,10}$	66.66	4.82	57.01	75.85	61.97	1.80	58.51	65.53	61.91	1.84	58.33	65.58
$P_{MHU,10}$	24.59	6.14	13.00	37.15	28.08	7.17	15.14	42.57	31.68	7.15	18.34	46.70
$E_{MHU,10}$	91.58	5.80	80.49	102.90	88.62	6.44	76.22	101.17	84.90	6.31	72.91	97.52
$R_{MHU,10}$	19.97	3.47	13.51	27.28	21.64	3.96	14.56	29.96	23.35	4.13	15.60	31.66
$Q_{MHU,10}$	129.83	3.89	122.55	137.63	118.56	1.60	115.43	121.65	118.31	1.63	115.15	121.62
$P_{SUP,101}$	109.59	7.57	94.81	124.36	95.58	8.02	80.25	111.27	98.99	8.00	82.99	114.95
$E_{SUP,101}$	1.31	3.34	-5.37	7.75	2.80	3.28	-3.40	9.36	2.42	3.31	-3.90	9.05
$R_{SUP,101}$	178.75	6.32	165.44	190.24	166.60	7.85	150.24	180.91	171.56	7.54	156.37	185.58
$Q_{SUP,101}$	56.61	4.28	48.42	65.32	51.68	1.71	48.36	55.08	51.53	1.74	48.15	54.96
$P_{MHU,101}$	90.60	6.95	76.64	104.32	81.48	7.40	67.22	95.56	85.29	7.63	70.69	100.32
$E_{MHU,101}$	-0.66	3.01	-6.54	5.32	0.21	3.06	-5.94	6.16	-0.16	3.12	-6.28	6.08
$R_{MHU,101}$	132.20	4.91	122.90	141.78	126.54	5.17	116.79	136.63	129.92	5.44	119.40	140.39
$Q_{MHU,101}$	120.16	3.87	113.07	128.10	113.73	1.54	110.75	116.85	113.46	1.53	110.44	116.46
$P_{SUP,113}$	85.72	8.02	70.16	101.75	77.04	8.10	60.91	92.57	80.12	8.42	63.93	96.47
$E_{SUP,113}$	-4.74	3.47	-11.49	2.05	-3.98	3.34	-10.31	2.90	-4.28	3.31	-10.69	2.43
$R_{SUP,113}$	165.55	11.63	142.87	188.04	148.18	12.49	124.26	172.95	153.13	12.95	128.21	178.71
$Q_{SUP,113}$	82.30	4.25	74.29	90.90	77.33	1.67	73.97	80.63	77.21	1.72	73.72	80.60
$P_{MHU,113}$	85.26	7.73	70.19	100.71	80.70	8.21	64.92	97.11	84.11	8.20	67.99	100.04
$E_{MHU,113}$	-6.81	3.16	-12.93	-0.44	-6.72	3.08	-12.51	-0.64	-6.81	3.14	-12.80	-0.79
$R_{MHU,113}$	134.12	10.90	113.24	156.45	129.10	11.43	107.10	152.20	133.63	11.38	111.09	156.16
$Q_{MHU,113}$	126.45	3.84	119.27	134.40	119.93	1.51	117.00	122.89	119.72	1.50	116.86	122.74

Table 6. Monte Carlo statistics – mean, standard deviation (S.D.), 2.5% and 97.5% quantiles – for select inferred water balance component parameters (in millimeters). We present the inferred parameters for October 2005 ($t = 10$), May 2013 ($t = 101$), and May 2014 ($t = 113$).
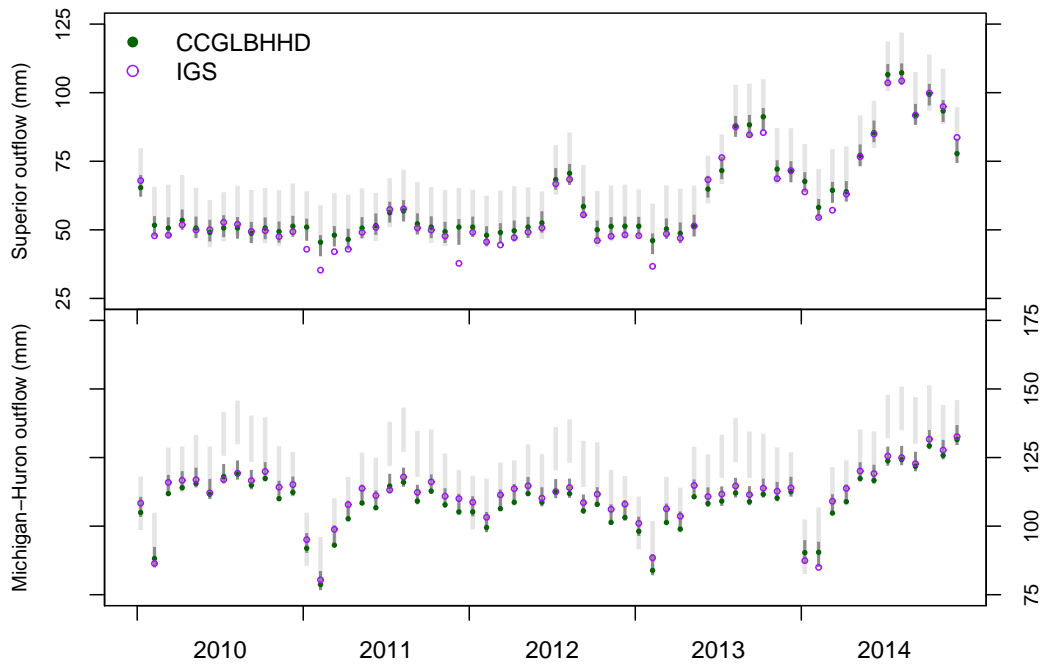
Figure 5. Representative estimates (95% credible intervals) of flow (in mm over the respective lake surface) through the connecting channels from Lake Superior (i.e. St. Marys River) and from Lake Michigan-Huron (i.e. St. Clair River) from the prototype L2SWBM (light grey bars) and experimental L2SWBM f12FF (dark grey bars). Historical flow measurements are represented by solid dots (CCGLBHHD) and circles (IGS).
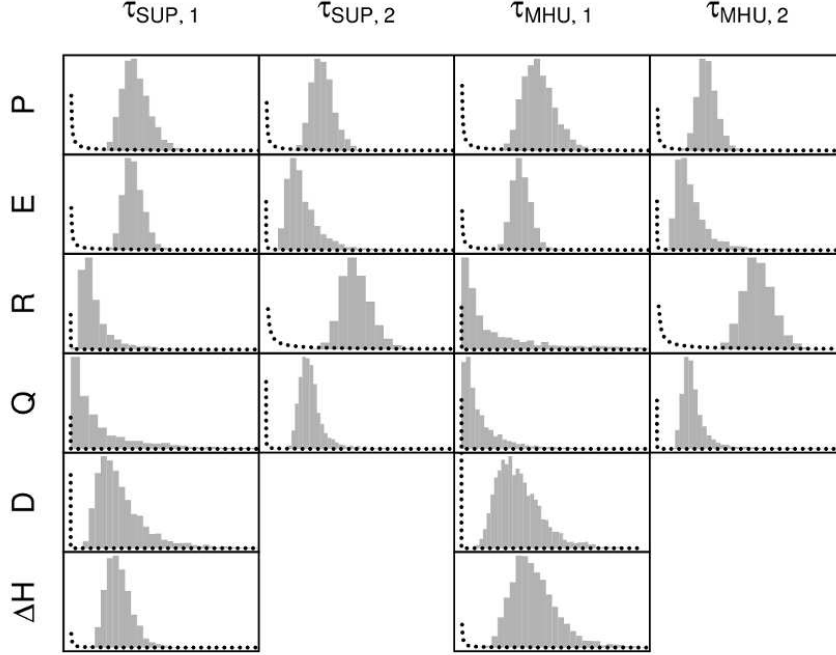
Figure 6. Comparison of vague Gamma priors (dotted lines) and inferred posterior histograms (gray bars) for the precision of input estimates for Lakes Superior and Michigan-Huron's water balance parameters. Plots utilize representative MCMC samples drawn for model f12FF. Rows represent individual balance parameters and columns indicate which lake and input estimate for τ is plotted. Subscript θ for column labels is omitted. Priors were non-informative for approximately 16/20 or 80% of precision parameters.

ance component estimates' $(\tau_{l,\theta,n})$ were, for the most part, non-informative in our selected models. Figure 6 shows that, for more than half of the τ parameters in model f12FF, the MCMC samples of the posterior distribution appear approximately normal in great contrast to the prior Gamma distribution applied. Table 7 further supports the vague priors as non-informative, listing the inferred precisions as standard deviations. None of the inferred precisions are, on average, significantly low. Notably, LBRM estimates were inferred to be more imprecise compared to other water balance component estimates, and inferred precisions for ARM estimates were sharply higher, possibly highlighting better accuracy of stream-gauge based over model-based estimates of runoff into large lakes. Additionally, constraining bias on channel flow and diversion estimates did not result in significantly lower inferred precisions for the same estimates, comparing the prototype and experimental L2SWBMs.

Inferred seasonal biases for independent water balance component estimates $\eta_{l,\theta,n,c(t)}$ were not strongly influenced by their vague $\mathsf{N}(0, 0.01)$ priors (figure 7). While data support negligible bias over the late spring and early summer for estimates of all components of the water balance, strong biases were inferred for the cooler fall, winter, and spring months. Many factors may explain the inferred biases, including inaccurate, land-based precipitation measurements in freezing or snowy conditions, poor representation of lake thermodynamics for evaporation estimates, frozen streams interfering with the accurate measurement of surface runoff into the lakes, and (despite constrained bias priors for $\eta_{l,\zeta,n,c(t)}$) a lack of compensation for ice jams in channel flow measurements.

24

Parameter	PROT			f12NF			f12FF		
	Mean	2.5%	97.5%	Mean	2.5%	97.5%	Mean	2.5%	97.5%
$\sigma_{SUP,P,1}$	9.90	12.09	8.19	9.60	11.82	7.89	9.66	12.02	7.90
$\sigma_{SUP,P,2}$	9.99	12.16	8.27	10.32	12.65	8.61	10.43	12.61	8.72
$\sigma_{SUP,E,1}$	9.54	11.32	8.14	9.80	11.53	8.47	9.84	11.60	8.48
$\sigma_{SUP,E,2}$	4.67	6.65	3.18	4.02	6.11	2.62	4.01	6.06	2.64
$\sigma_{SUP,R,1}$	1.85	6.10	0.65	2.36	6.59	1.08	2.81	7.00	1.88
$\sigma_{SUP,R,2}$	14.57	17.20	12.54	14.17	16.82	12.09	13.90	16.44	11.89
$\sigma_{SUP,Q,1}$	0.50	2.31	0.22	0.49	2.13	0.22	0.50	2.04	0.23
$\sigma_{SUP,Q,2}$	2.76	3.61	1.99	2.87	3.72	2.26	2.94	3.72	2.26
$\sigma_{SUP,D,1}$	0.78	1.25	0.49	0.76	1.22	0.47	0.77	1.24	0.49
$\sigma_{SUP,\Delta H,w}$	10.06	12.94	8.06	11.17	14.60	8.71	11.18	14.47	8.76
$\sigma_{MHU,P,1}$	8.84	10.91	7.25	8.81	10.92	7.25	8.83	10.97	7.25
$\sigma_{MHU,P,2}$	10.56	12.82	8.80	10.94	13.33	9.17	11.04	13.48	9.23
$\sigma_{MHU,E,1}$	10.06	11.81	8.64	10.04	11.82	8.67	10.06	11.85	8.70
$\sigma_{MHU,E,2}$	3.23	6.14	2.10	3.42	6.27	2.17	3.71	6.36	2.29
$\sigma_{MHU,R,1}$	0.67	3.89	0.26	0.66	4.19	0.27	0.69	4.15	0.27
$\sigma_{MHU,R,2}$	13.60	15.91	11.91	13.34	15.66	11.61	13.25	15.50	11.49
$\sigma_{MHU,Q,1}$	0.47	1.59	0.22	0.47	1.64	0.21	0.48	1.66	0.22
$\sigma_{MHU,Q,2}$	1.41	2.06	0.82	1.29	2.02	0.70	1.36	2.03	0.76
$\sigma_{MHU,D,1}$	0.18	0.27	0.12	0.18	0.27	0.12	0.18	0.27	0.13
$\sigma_{MHU,\Delta H,w}$	8.62	11.28	6.77	9.02	12.57	6.63	9.14	12.65	6.81

Table 7. Monte Carlo statistics for the inferred precisions from L2SWBMs PROT, f12NF, and f12FF, shown as standard deviations (in millimeters), with the 2.5 percentile being the high part of the 95% credible interval, and the 97.5 percentile being the low part of the 95% credible interval.
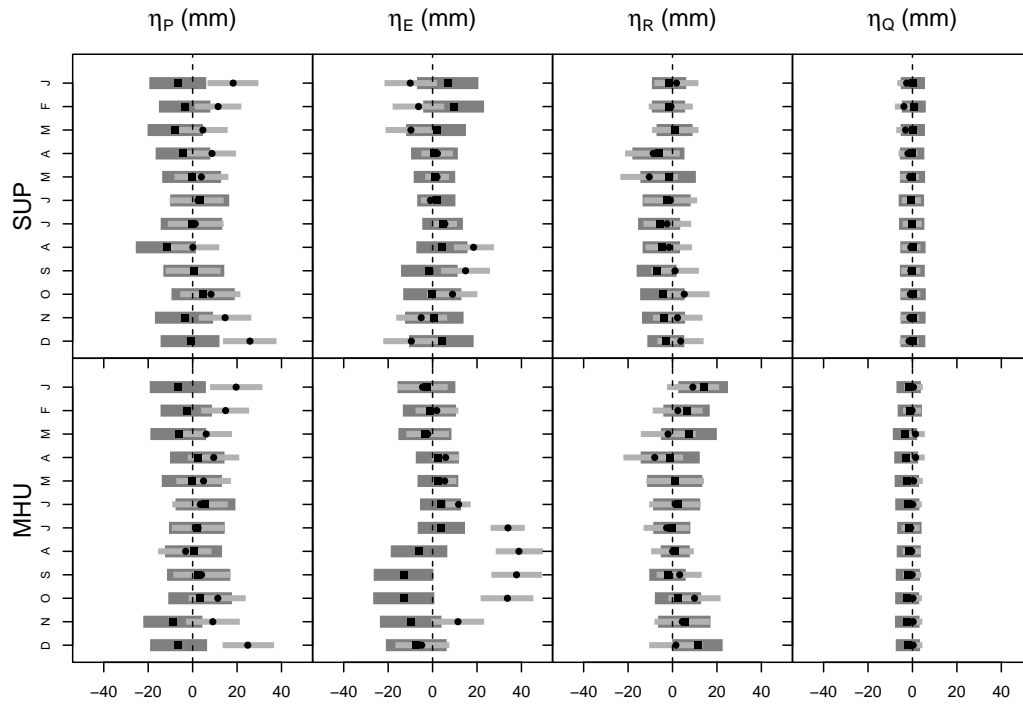
Figure 7. Inferred biases via MCMC samples for model f12FF of independent water balance estimates for (respective of the column labels at the top of the figure) precipitation, evaporation, runoff, and channel outflow for Lakes Superior and Michigan-Huron. Each tick along the vertical axes represents a calendar month, while the bias value is represented along the horizontal axes. Dark gray bars represent the biases' inferred 95% credible interval for the first set $(n = 1)$ of independent estimates for each component, while light gray bars represent the biases' inferred 95% credible interval for the second set $(n = 2)$ of independent estimates. Black squares correspond to the mean inferred bias for the first set $(n = 1)$ of independent estimates for each component, while black dots correspond to the mean inferred bias for the second set $(n = 2)$ of independent estimates.

4.3. Future work

The experiment described in this paper led to the evolution of an L2SWBM for the Laurentian Great Lakes, and has the potential to support the development of similar L2SWBMs for other large lake systems around the world. The experiment design can be modified to experiment with other inference windows and error structures. Expansion of the new model (or models) to Lakes St. Clair, Erie, and Ontario, as well as back in time to 1950, is expected to be non-trivial. The number of parameters to estimate and required computation time will increase, and there will be other factors to consider, such as water flow through the Huron-Erie Corridor, and meteorological station and stream gauge availability over time. As the models are tested and improved, possibly with different model structures, we expect that the resulting water balance component estimates will be employed not only by water management authorities, but will be distributed to the public as well through (among other interfaces) the NOAA Great Lakes Dashboard Project [13, 32, 68].

5. Supplementary material

Supplementary material related to this article can be found with the on-line version of this journal article. Plots of time series of inferred water balance components from the prototype, model f12NF, and model f12FF are included. Additionally, compressed folders containing Superior and Michigan-Huron L2SWBM code and data may be downloaded from https://www.glerl.noaa.gov/data/WaterBalanceModel/. Necessary software packages are available for all major computing platforms (e.g. Windows, Mac, and Linux).

6. Acknowledgements

A preprint of this article is available. See [67].

References

[1] F.S. Ahrestani, M. Hebblewhite, and E. Post, *The importance of observation versus process error in analyses of global ungulate populations*, Scientific reports 3 (2013), p. 3125.

[2] C. Armero, A. Lopez-Quilez, and R. Lopez-Sanchez, *Bayesian assessment of times to diagnosis in breast cancer screening*, Journal of Applied Statistics 35 (2008), pp. 997–1009.

[3] N.W. Arnell, *A simple water balance model for the simulation of streamflow over a large geographic domain*, Journal of Hydrology 217 (1999), pp. 314–335.

[4] J.G. Arnold, R. Srinivasan, R.S. Muttiah, and J.R. Williams, *Large area hydrologic modeling and assessment part I: Model development* (1998).

[5] B.C. Bates and E.P. Campbell, *A Markov chain Monte Carlo scheme for parameter estimation and inference in conceptual rainfall-runoff modeling*, Water resources research 37 (2001), pp. 937–947.

[6] K.K. Benke, K.E. Lowell, and A.J. Hamilton, *Parameter uncertainty, sensitivity analysis and prediction error in a water-balance hydrological model*, Mathematical and Computer Modelling 47 (2008), pp. 1134–1149.

[7] M. Blangiardo and G. Baio, *Evidence of bias in the eurovision song contest: modelling the votes using bayesian hierarchical models*, Journal of Applied Statistics 41 (2014), pp. 2312–2322.

[8] M.E. Borsuk, R. Clemen, L. Maguire, and K.H. Reckhow, *Stakeholder values and scientific modeling in the Neuse River watershed*, Group Decision and Negotiation 10 (2001), pp. 355–373.

[9] W. Boughton, *The Australian water balance model*, Environmental Modelling & Software 19 (2004), pp. 943–956.

[10] S.P. Brooks and A. Gelman, *General methods for monitoring convergence of iterative simulations*, Journal of Computational and Graphical Statistics 7 (1998), pp. 434–455.

[11] N. Bulygina and H. Gupta, *Estimating the uncertain mathematical structure of a water balance model via bayesian data assimilation*, Water Resources Research 45 (2009).

[12] CCGLBHHD, *Coordinated Great Lakes physical data*, Tech. Rep., Coordinating Committee on Great Lakes Basic Hydraulic and Hydrologic Data, 1977. Available at www.lre.usace.army.mil/.

[13] A.H. Clites, J.P. Smith, T.S. Hunter, and A.D. Gronewold, *Visualizing relationships between hydrology, climate, and water level fluctuations on Earth's largest system of lakes*, Journal of Great Lakes Research 40 (2014), pp. 807–811.

[14] T.E. Croley, *Verifiable evaporation modeling on the laurentian great lakes*, Water Resources Research 25 (1989), pp. 781–792.

[15] T.E. Croley, *Long-term heat storage in the great lakes*, Water resources research 28 (1992), pp. 69–81.

[16] T.E. Croley and H.C. Hartmann, *Resolving thiessen polygons*, Journal of Hydrology 76 (1985), pp. 363–379.

[17] T.E. Croley and C. He, *Distributed-parameter large basin runoff model. I: Model development*, Journal of Hydrologic Engineering 10 (2005), pp. 173–181.

[18] W.T. Crow, W.P. Kustas, and J.H. Prueger, *Monitoring root-zone soil moisture through the assimilation of a thermal remote sensing-based soil moisture proxy into a water balance model*, Remote Sensing of Environment 112 (2008), pp. 1268–1281.

[19] D. Deacu, V. Fortin, E. Klyszejko, C. Spence, and P.D. Blanken, *Predicting the net basin*

supply to the Great Lakes with a hydrometeorological model, Journal of Hydrometeorology 13 (2012), pp. 1739–1759.

[20] S. Dorner, J. Shi, and D. Swayne, *Multi-objective modelling and decision support using a Bayesian network approximation to a non-point source pollution model*, Environmental Modelling & Software 22 (2007), pp. 211–222.

[21] L.E. Eberly, B.P. Carlin, *et al.*, *Identifiability and convergence issues for Markov chain Monte Carlo fitting of spatial models*, Statistics in medicine 19 (2000), pp. 2279–2294.

[22] K. Engeland and L. Gottschalk, *Bayesian estimation of parameters in a regional hydrological model*, Hydrology and Earth System Sciences Discussions 6 (2002), pp. 883–898.

[23] K. Engeland, C.Y. Xu, and L. Gottschalk, *Assessing uncertainties in a conceptual water balance model using bayesian methodology/estimation bayésienne des incertitudes au sein dune modélisation conceptuelle de bilan hydrologique*, Hydrological Sciences Journal 50 (2005).

[24] L. Fry, T. Hunter, M. Phanikumar, V. Fortin, and A. Gronewold, *Identifying streamgage networks for maximizing the effectiveness of regional water balance modeling*, Water Resources Research 49 (2013), pp. 2689–2700.

[25] A. Gelman, *How to think about identifiability in Bayesian inference*, http://andrewgelman.com/2014/02/12/think-identifiability-bayesian-inference/ (2014).

[26] A. Gelman and D.B. Rubin, *Inference from iterative simulation using multiple sequences*, Statistical Science 7 (1992), pp. 457–472.

[27] A. Gelman and C.R. Shalizi, *Philosophy and the practice of Bayesian statistics*, British Journal of Mathematical and Statistical Psychology 66 (2013), pp. 8–38.

[28] J. Gibson, T. Prowse, and D. Peters, *Hydroclimatic controls on water balance and water level variability in Great Slave Lake*, Hydrological Processes 20 (2006), pp. 4155–4172.

[29] J. Gill, *Is partial-dimension convergence a problem for inferences from MCMC algorithms?*, Political Analysis 16 (2007), pp. 153–178.

[30] A.D. Gronewold, J. Bruxer, D. Durnford, J.P. Smith, A.H. Clites, F. Seglenieks, S.S. Qian, T.S. Hunter, and V. Fortin, *Hydrological drivers of record-setting water level rise on Earth's largest lake system*, Water Resources Research 52 (2016), pp. 4026–4042.

[31] A.D. Gronewold, A.H. Clites, J. Bruxer, K. Kompoltowicz, J.P. Smith, T.S. Hunter, and C. Wong, *Water levels surge on Great Lakes*, Eos, Transactions American Geophysical Union 96 (2015), pp. 14–17.

[32] A.D. Gronewold, A.H. Clites, J.P. Smith, and T.S. Hunter, *A dynamic graphical interface for visualizing projected, measured, and reconstructed surface water elevations on the Earth's largest lakes*, Environmental Modelling and Software 49 (2013), pp. 34–39.

[33] A.D. Gronewold, V. Fortin, B.M. Lofgren, A.H. Clites, C.A. Stow, and F.H. Quinn, *Coasts, water levels, and climate change: A Great Lakes perspective*, Climatic Change 120 (2013), pp. 697–711.

[34] S. Guo, J. Wang, L. Xiong, A. Ying, and D. Li, *A macro-scale and semi-distributed monthly water balance model to predict climate change impacts in China*, Journal of Hydrology 268 (2002), pp. 1–15.

[35] K. Holman, A. Gronewold, M. Notaro, and A. Zarrin, *Improving historical precipitation*

estimates over the lake superior basin, Geophysical Research Letters 39 (2012).

[36] T.S. Hunter, A.H. Clites, K.B. Campbell, and A.D. Gronewold, *Development and application of a North American Great Lakes hydrometeorological database Part I: Precipitation, evaporation, runoff, and air temperature*, Journal of Great Lakes Research 41 (2015), pp. 65–77.

[37] G.J. Husak, J. Michaelsen, and C. Funk, *Use of the gamma distribution to represent monthly rainfall in Africa for drought monitoring applications*, International Journal of Climatology 27 (2007), pp. 935–944.

[38] T.E.C. II and R.A. Assel, *A one-dimensional ice thermodynamics model for the Laurentian Great Lakes*, Water Resources Research 30 (1994), pp. 625–639.

[39] K.R. Jin, J.H. Hamrick, and T. Tisdale, *Application of three-dimensional hydrodynamic model for Lake Okeechobee*, Journal of Hydraulic Engineering 126 (2000), pp. 758–771.

[40] X. Jin, C.Y. Xu, Q. Zhang, and V. Singh, *Parameter and modeling uncertainty simulated by glue and a formal bayesian method for a conceptual hydrological model*, Journal of Hydrology 383 (2010), pp. 147–155.

[41] J. Joseph and J.H. Guillaume, *Using a parallelized MCMC algorithm in R to identify appropriate likelihood functions for SWAT*, Environmental Modelling & Software 46 (2013), pp. 292–298.

[42] S. Kebede, Y. Travi, T. Alemayehu, and V. Marc, *Water balance of Lake Tana and its sensitivity to fluctuations in rainfall, Blue Nile basin, Ethiopia*, Journal of Hydrology 316 (2006), pp. 233–247.

[43] C. Kim and J. Stricker, *Influence of spatially variable soil hydraulic properties and rainfall intensity on the water budget*, Water Resources Research 32 (1996), pp. 1699–1712.

[44] J.K. Kruschke, *Posterior predictive checks can and should be Bayesian: Comment on Gelman and Shalizi, 'Philosophy and the practice of Bayesian statistics'*, British Journal of Mathematical and Statistical Psychology 66 (2013), pp. 45–56.

[45] F. Lespinas, V. Fortin, G. Roy, P. Rasmussen, and T. Stadnyk, *Performance evaluation of the Canadian Precipitation Analysis (CaPA)*, Journal of Hydrometeorology 16 (2015), pp. 2045–2064.

[46] X.Y. Li, H.Y. Xu, Y.L. Sun, D.S. Zhang, and Z.P. Yang, *Lake-level change and water balance analysis at Lake Qinghai, West China during recent decades*, Water Resources Management 21 (2007), pp. 1505–1516.

[47] D. Lunn, D. Spiegelhalter, A. Thomas, and N. Best, *The BUGS project: Evolution, critique and future directions*, Statistics in Medicine 28 (2009), pp. 3049–3067.

[48] D.J. Lunn, A. Thomas, N. Best, and D. Spiegelhalter, *WinBUGS-a Bayesian modelling framework: concepts, structure, and extensibility*, Statistics and Computing 10 (2000), pp. 325–337.

[49] Z. Makhlouf and C. Michel, *A two-parameter monthly water balance model for French watersheds*, Journal of Hydrology 162 (1994), pp. 299–318.

[50] O. Malve, M. Laine, H. Haario, T. Kirkkala, and J. Sarvala, *Bayesian modelling of algal mass occurrencesusing adaptive MCMC methods with a lake water quality model*, Environmental Modelling & Software 22 (2007), pp. 966–977.

[51] G. Martine, G. McGranahan, M. Montgomery, and R. Fernandez-Castilla, *The New Global*

Frontier: Urbanization, Poverty, and Environment in the 21st Century, Routledge Earthscan, New York, NY, 2008.

[52] P.C. Milly, J. Betancourt, M. Falkenmark, R.M. Hirsch, Z.W. Kundzewicz, D.P. Lettenmaier, and R.J. Stouffer, *Stationarity is dead: whither water management?*, Science 319 (2008), pp. 573–574.

[53] D.C. Montgomery, *Design and Analysis of Experiments*, John Wiley & Sons, 2008.

[54] S. Mouelhi, C. Michel, C. Perrin, and V. Andréassian, *Stepwise development of a two-parameter monthly water balance model*, Journal of Hydrology 318 (2006), pp. 200–214.

[55] D.S. Mueller, J.D. Abad, C.M. Garcia, J.W. Gartner, M.H. Garcia, and K.A. Oberg, *Errors in acoustic Doppler profiler velocity measurements caused by flow disturbance*, Journal of Hydraulic Engineering 133 (2007), pp. 1411–1420.

[56] M. Pan and E.F. Wood, *Data assimilation for estimating the terrestrial water budget using a constrained ensemble Kalman filter*, Journal of Hydrometeorology 7 (2006), pp. 534–547.

[57] H.L. Penman, *Natural evaporation from open water, bare soil and grass*, in *Proc. R. Soc. Lond. A*, Vol. 193. The Royal Society, 1948, pp. 120–145.

[58] B. Piper, D. Plinston, and J. Sutcliffe, *The water balance of Lake Victoria*, Hydrological Sciences Journal 31 (1986), pp. 25–37.

[59] M. Plummer, *et al.*, *JAGS: A program for analysis of Bayesian graphical models using Gibbs sampling*, in *Proceedings of the 3rd international workshop on distributed statistical computing*, Vol. 124. Vienna, 2003, p. 125.

[60] F.H. Quinn and B. Guerra, *Current perspectives on the Lake Erie water balance*, Journal of Great Lakes Research 12 (1986), pp. 109–116.

[61] R Core Team, *R: A language and environment for statistical computing*, R Foundation for Statistical Computing, Vienna, Austria (2014).

[62] D. Raes, S. Geerts, E. Kipkorir, J. Wellens, and A. Sahli, *Simulation of yield decline as a result of water stress with a robust soil water balance model*, Agricultural Water Management 81 (2006), pp. 335–357.

[63] B. Rannala, *Identifiability of parameters in mcmc bayesian inference of phylogeny*, Systematic Biology 51 (2002), pp. 754–760.

[64] B. Renard, D. Kavetski, G. Kuczera, M. Thyer, and S.W. Franks, *Understanding predictive uncertainty in hydrologic modeling: The challenge of identifying input and structural errors*, Water Resources Research 46 (2010).

[65] M. Rodell, J. Famiglietti, J. Chen, S. Seneviratne, P. Viterbo, S. Holl, and C. Wilson, *Basin scale estimates of evapotranspiration using GRACE and other observations*, Geophysical Research Letters 31 (2004).

[66] J. Sheffield, C.R. Ferguson, T.J. Troy, E.F. Wood, and M.F. McCabe, *Closing the terrestrial water budget from satellite remote sensing*, Geophysical Research Letters 36 (2009).

[67] J.P. Smith and A.D. Gronewold, *Development and analysis of a Bayesian water balance model for large lake systems*, ArXiv e-prints (2017).

[68] J.P. Smith, T.S. Hunter, A.H. Clites, C.A. Stow, T. Slawecki, G.C. Muhr, and A.D. Gronewold, *An expandable web-based platform for visually analyzing basin-scale hydro-climate time series data*, Environmental Modelling & Software 78 (2016), pp. 97–105.

[69] D.J. Spiegelhalter, N.G. Best, B.P. Carlin, and A. Linde, *The deviance information criterion: 12 years on*, Journal of the Royal Statistical Society: Series B (Statistical Methodology) 76 (2014), pp. 485–493.

[70] D.J. Spiegelhalter, N.G. Best, B.P. Carlin, and A. Van Der Linde, *Bayesian measures of model complexity and fit*, Journal of the Royal Statistical Society: Series B (Statistical Methodology) 64 (2002), pp. 583–639.

[71] S. Swenson and J. Wahr, *Monitoring the water balance of Lake Victoria, East Africa, from space*, Journal of Hydrology 370 (2009), pp. 163–176.

[72] H.C. Thom, *A note on the gamma distribution*, Monthly Weather Review 86 (1958), pp. 117–122.

[73] United States Geological Survey, *National Water Information Service*, Available at https://waterdata.usgs.gov/nwis/inventory (2017/02/20) (2017).

[74] A. Voinov and F. Bousquet, *Modelling with stakeholders*, Environmental Modelling and Software 25 (2010), pp. 1268–1281.

[75] C.J. Vörösmarty, C.A. Federer, and A.L. Schloss, *Potential evaporation functions compared on US watersheds: Possible implications for global-scale water balance and terrestrial ecosystem modeling*, Journal of Hydrology 207 (1998), pp. 147–169.

[76] C.J. Vörösmarty, P. Green, J. Salisbury, and R.B. Lammers, *Global water resources: vulnerability from climate change and population growth*, science 289 (2000), pp. 284–288.

[77] C.Y. Xu and V.P. Singh, *A review on monthly water balance models for water resources investigations*, Water Resources Management 12 (1998), pp. 20–50.